Atmos. Chem. Phys., 9, 4145–4156, 2009
www.atmos-chem-phys.net/9/4145/2009/

Atmospheric Chemistry and Physics

^{36}Cl bomb peak: comparison of modeled and measured data

U. Heikkilä[1,*], J. Beer[1], J. Feichter[2], V. Alfimov[3], H.-A. Synal[3], U. Schotterer[4], A. Eichler[4], M. Schwikowski[5], and L. Thompson[6]

[1]EAWAG, Dübendorf, Switzerland
[2]Max Planck Institute for Meteorology, Hamburg, Germany
[3]Federal Institute of Technology (ETH) Zurich/Paul Scherrer Institute, Villigen, Switzerland
[4]Division of Climate and Environmental Physics, Physics Institute, University of Bern, Switzerland
[5]Paul Scherrer Institute, Villigen, Switzerland
[6]School of Earth Sciences, The Ohio State University, USA
[*]now at: Bjerknes Centre for Climate Research, Bergen, Norway

Received: 18 August 2008 – Published in Atmos. Chem. Phys. Discuss.: 27 January 2009
Revised: 17 April 2009 – Accepted: 15 June 2009 – Published: 23 June 2009

Abstract. The extensive nuclear bomb testing of the fifties and sixties and the final tests in the seventies caused a strong ^{36}Cl peak that has been observed in ice cores worldwide. The measured ^{36}Cl deposition fluxes in eight ice cores (Dye3, Fiescherhorn, Grenzgletscher, Guliya, Huascarán, North GRIP, Inylchek (Tien Shan) and Berkner Island) were compared with an ECHAM5-HAM general circulation model simulation (1952–1972). We find a good agreement between the measured and the modeled ^{36}Cl fluxes assuming that the bomb test produced global ^{36}Cl input was ∼80 kg. The model simulation indicates that the fallout of the bomb test produced ^{36}Cl is largest in the subtropics and mid-latitudes due to the strong stratosphere-troposphere exchange. In Greenland the ^{36}Cl bomb signal is quite large due to the relatively high precipitation rate. In Antarctica the ^{36}Cl bomb peak is small but is visible even in the driest areas. The model suggests that the large bomb tests in the Northern Hemisphere are visible around the globe but the later (end of sixties and early seventies) smaller tests in the Southern Hemisphere are much less visible in the Northern Hemisphere. The question of how rapidly and to what extent the bomb produced ^{36}Cl is mixed between the hemispheres depends on the season of the bomb test. The model results give an estimate of the amplitude of the bomb peak around the globe.

1 Introduction

Atmospheric nuclear bomb tests which started in the fifties and continued until the late seventies put large amounts of radioactive material into the stratosphere. This anthropogenic input largely exceeded the natural levels and caused distinct peaks in deposition fluxes world-wide. These peaks can be used to test stratospheric transport and residence times of tracers (^{137}Cs, ^{90}Sr) (Lal and Peters, 1967), also in combination with atmospheric general circulation models (Rehfeld et al., 1995). They can also be used as tracers to study oceanic mixing (^{14}C) and groundwater dating (^{3}H, ^{36}Cl) (Schlosser et al., 1988; Davis et al., 2001). For the natural sources of ^{36}Cl we refer to Blinov et al. (2000).

The radionuclide ^{36}Cl has also been excessively produced during the nuclear bomb tests which were conducted in the vicinity of oceans, such as the tests that took place on islands, atolls or barges. The neutrons, released by the nuclear reactions, activate the ^{35}Cl of the sea salt and produce the ^{36}Cl isotope (^{35}Cl(n,γ)^{36}Cl). The amount of the ^{36}Cl produced by the tests exceeded the natural production by a factor of ∼1000.

The measured "bomb peak" of ^{36}Cl in Greenland at Dye3 site has been published earlier by Elmore et al. (1982) and Synal et al. (1990). Synal et al. (1990) used an atmospheric 4-box model to simulate the fall-out pattern of the stratospheric ^{36}Cl in Greenland. They succeeded in obtaining the shape of the fall-out curve by assuming a stratospheric residence time of 2.0±0.3 years for ^{36}Cl.

Correspondence to: U. Heikkilä
(ulla.heikkilae@eawag.ch)

Published by Copernicus Publications on behalf of the European Geosciences Union.

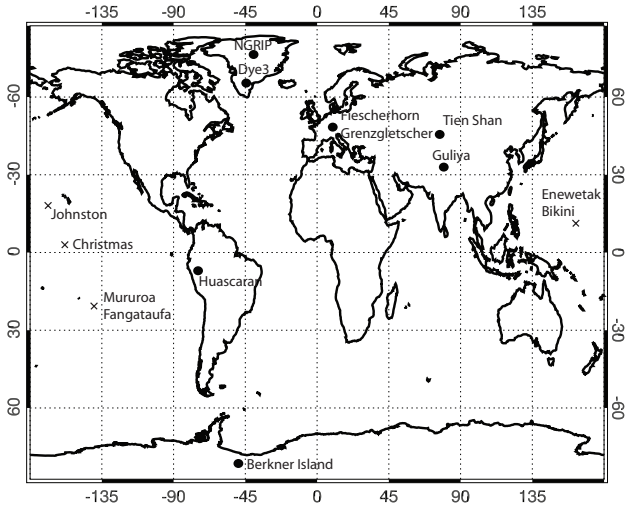

Fig. 1. The location of the bomb tests, marked with crosses, which produced ^{36}Cl: Enewetak and Bikini atolls, Johnston and Christmas Islands and Mururoa and Fangataufa atolls. The location of the eight ice cores, marked with points, investigated in this study: NGRIP and Dye3 in Greenland, Fiescherhorn and Grenzgletscher in the Alps, Guliya and Tien Shan in Asia, Huascarán in the Andes and Berkner Island in Antarctica.

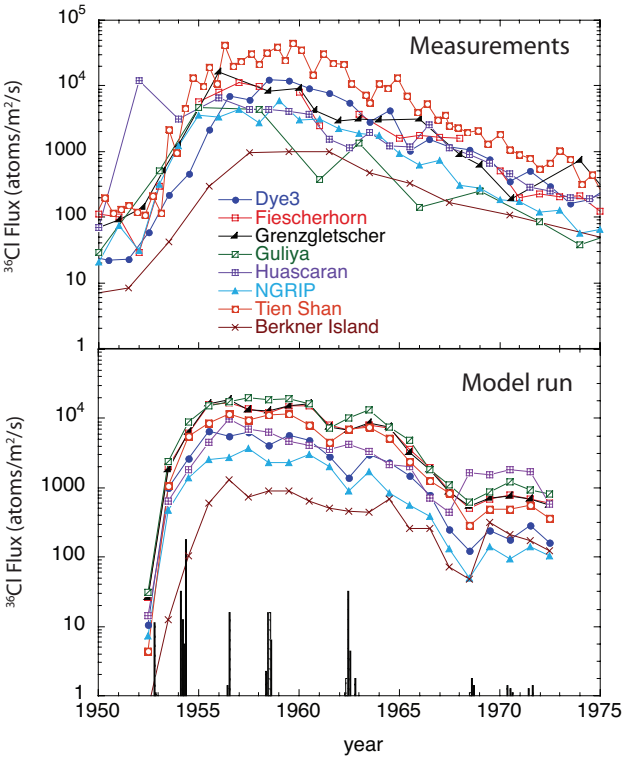

Fig. 2. The measured (above) and modeled (below) peaks of ^{36}Cl deposition fluxes at eight ice core sites. The vertical lines in the lower figure show the bomb test input of ^{36}Cl according to Table 1. Their amplitude shows the strength of the bomb test but is not to scale with the deposition fluxes.

Data from other ice cores exist in which the ^{36}Cl concentrations were measured. These cores were drilled in the Guliya ice cap in the Himalayas, in Huascarán in the Andes, in Fiescherhorn and Grenzgletscher in the Alps in Switzerland, in northern Greenland, the North GRIP ice core (NGRIP), a Kyrgyz ice core from the Inylchek glacier of the Tien Shan mountains and an Antarctic core from the Berkner Island. See Sect. 2 for details and Fig. 1 for their location. The measured deposition fluxes of ^{36}Cl in these locations are shown in Fig. 2. All these fluxes show a very similar fall-out pattern but show some differences regarding amplitude and timing.

We utilize this data to study the deposition distribution of the bomb-produced ^{36}Cl with the atmospheric general circulation model ECHAM5-HAM. The following questions are addressed: 1) Are there differences in the amplitude of the peaks and are these related to the location of the ice core or climatic conditions, such as the precipitation rate at the site? 2) Is the shift in the maxima of the peaks related to transport processes or rather to uncertainties in the dating of the cores? and 3) How well does the model perform in reproducing the stratospheric transport and stratosphere-troposphere exchange of ^{36}Cl?

2 Observed ^{36}Cl bomb peaks in ice cores

Details of the drilling of the ice cores as well as other measured parameters have been published earlier: Dye3 (including ^{36}Cl) by Synal et al. (1990), Fiescherhorn glacier by Schotterer et al. (1997a), Grenzgletscher by Eichler et al. (2000), Guliya by Thompson et al. (1995a), Huascarán by Thompson et al. (1995b), NGRIP by Andersen et al. (2006); North Greenland Ice Core Project Members (2004) and Inylchek (Tien Shan) by Green et al. (2004). Details of the ice core from the Berkner Island have not been published earlier. The ^{36}Cl concentrations in ice analyzed in this study were all measured at the Accelerator Mass Spectrometer facility of ETH Zurich/PSI. We refer to the references for details of calculating the ^{36}Cl deposition fluxes.

Due to the lack of an independent time scale for Inylchek (Tien Shan) ice core, a rough chronology has been developed. The sharp forward slope of the bomb peak was assigned to the year 1954 when the first major explosions took place, and a linear accumulation rate was assumed.

The ^{36}Cl bomb peak in a couple of other locations has also been measured at EAWAG and ETH/PSI: the Vostok snow pit in Antarctica (Delmas et al., 2004) and the Kilimanjaro ice core in Africa (Thompson et al., 2002) (the ^{36}Cl profile is available in the supporting online information). Both areas are extremely dry. It was found that the shape of the bomb peaks in these cores was very different from the cores shown in this work, which is why these results were not used for

the analysis. The concentrations at Vostok and Kilimanjaro reached the maximum some 10 years later than in the other cores and the fallout was much slower so that no real peak could be observed. Delmas et al. (2004) explained this by sublimation of ^{36}Cl in the form of HCl in the firn which is still connected to the atmosphere. This is especially a problem in ice cores with extremely low accumulation rate but ice cores at high accumulation areas should not be influenced by it. Röthlisberger et al. (2003) specified a value of 0.1 mm/day (4 g/cm^2/yr or 4 mm water equivalent (W.E.)/yr) without a strong seasonality above which the effect of sublimation of gaseous ^{36}Cl should be negligible. The ^{36}Cl deposition flux measured in the Berkner Island ice core seems to be slightly influenced by this phenomenon because the maximum is reached some years later than in other cores and the fallout after the maximum is flatter and the flux has not reached the natural level in the end of the experiment (see the measured flux in Fig. 2). The precipitation rate on Berkner Island is quite low (0.3±0.3 mm/day) which is larger than the limit of 0.1 mm/day estimated by Röthlisberger et al. (2003) however the seasonality is large. The sublimation of the gaseous ^{36}Cl in the Berkner Island core is not as severe as in the Vostok and Kilimanjaro cores because a steep peak is visible. We include this core in our analysis keeping in mind the sublimation effect.

Table 2 shows the integrated total masses of the measured ice core bomb peaks of ^{36}Cl. The fallout slopes of ^{36}Cl were estimated by line fitting on logarithmic scale. Table 2 shows the atmospheric residence times corresponding to these slopes. They vary between 3–5 years but some of them include large uncertainty because of the small number of data points, such as the Guliya ice core record. The uncertainty is probably in the order of ±1 year.

The obtained residence times are overestimated in comparison with the actual atmospheric residence times of ^{36}Cl because of the additional bomb tests which regularly put new ^{36}Cl into the stratosphere flattening the fall-out curve. Synal et al. (1990) estimated a residence time of 2±0.3 years from the Dye3 data between 1960 and 1964, during which no new tests took place.

3 Modeling of the ^{36}Cl bomb peaks

3.1 Model description and setup

The model employed for this study was the ECHAM5-HAM general circulation model. ECHAM5 is a fifth-generation atmospheric global circulation model (GCM) developed at the Max Planck Institute for Meteorology, Hamburg, evolving originally from the European Centre of Medium Range Weather Forecasts (ECWMF) spectral weather prediction model. It solves the prognostic equations for vorticity, divergence, surface pressure and temperature, expressed in terms of spherical harmonics with a triangular truncation. Non-linear processes and physical parametrizations are solved on a Gaussian grid. A complete description of the ECHAM5 GCM is given in Roeckner et al. (2003). The additional aerosol module HAM includes the microphysical processes, the emission and deposition of aerosols, a sulfur chemistry scheme and the radiative property scheme of the aerosols (Stier et al., 2005). We used present-day aerosol emissions from the AEROCOM emission inventory representative for the year 2000, described in Dentener et al. (2006). For this study a middle-atmospheric model version with a horizontal resolution of T42 (2.8×2.8 degrees) with 39 vertical levels up to 0.01 hPa (∼80 km) was used. The run was allowed to spin up for five years to let ^{36}Cl reach equilibrium and the years 1952–1972 were used for the analysis. The run was forced with prescribed observational monthly mean sea surface temperatures and sea ice cover obtained from the international model intercomparison AMIP2 project (Gates, 1992). We refer to Hagemann et al. (2006) for a detailed discussion on ECHAM5-HAM's ability to reproduce observed precipitation rates.

The natural production rates of ^{36}Cl were taken from the revised production rate calculations of Masarik and Beer (1999). The profiles were interpolated as a function of latitude and altitude using the monthly mean solar modulation function Φ reconstructed by Usoskin et al. (2005) and corrected for the local interstellar spectrum as in Steinhilber et al. (2008) for the years 1952–1972. However, the natural production of ^{36}Cl is much lower than the bomb produced ^{36}Cl and is not of importance during the modeled years. ECHAM5-HAM's ability to reproduce the observed concentrations and deposition fluxes of two other cosmogenic radionuclides ^{10}Be and ^{7}Be world-wide has been discussed at length in Heikkilä et al. (2008a).

The geochemical behaviour of ^{36}Cl is somewhat different from that of ^{10}Be or ^{7}Be. Like these two radionuclides, ^{36}Cl can become attached to aerosols and be transported and deposited with them. However, ^{36}Cl can also be present as HCl gas. How much of the ^{36}Cl is in particulate or gaseous form is not very well understood and depends on the chemical properties of the atmosphere. In the stratosphere we can assume the ^{36}Cl to be mostly gaseous as HCl (Zerle et al. (1997), Sachsenhauser et al.[1], T. Peter, personal communication). In the troposphere, especially in the lower layers, the situation is more complicated because ^{36}Cl can be present in both gaseous and particulate form. The deposition of the gaseous ^{36}Cl is somewhat different than that of particulate ^{36}Cl. The gases have a higher diffusion constant which leads to an increased dry deposition. Unfortunately the partitioning between gaseous and particulate phases of ^{36}Cl is not well understood and is probably also highly variable in space and time (Lukasczyk, 1994). Nevertheless, wet deposition is the dominant removal process both for gaseous and particulate

[1]Sachsenhauser, H., Zerle, L., Beer, J., Masarik, J., and Nolte, E.: Atmospheric transport of cosmogenic radionuclides, Wengen

^{36}Cl. For this reason, and because the transport of gas and particles is very similar, we treated all ^{36}Cl in the model as particulate and attached to aerosols.

3.2 Atmospheric bomb input of ^{36}Cl

The first bomb tests that produced large amounts of ^{36}Cl started in 1952. They were carried out by the US at the Enewetak (11.35° N, 162.35° E) and Bikini (11.30° N, 165.30° E) atolls in the Pacific ocean. These tests took place during the years 1952, 1954, 1956 and 1958. They were followed by the U.S. tests on the Christmas (2.00° N, 157.25° W) and Johnston (17.18° N, 169.45° W) islands in 1962. After the test ban treaty in 1963 some more ^{36}Cl-producing tests carried out by France took place in 1968 at Mururoa (21.50° S, 138.55° W) and Fangataufa (22.15° S, 138.45° W) atolls in 1968, 1970 and 1971. The locations of the test sites are shown in Fig. 1.

The details of the tests were obtained from http://www.iss.niiit.ru/ksenia/catal_nt/index.htm and http://www.radiochemistry.org/history/nuke_tests/pdf/NuclearExplosionsCatalog.pdf. The tests were catalogued with respect to their type (balloon, shaft, air drop etc.) which influences the amount of ^{36}Cl produced. Unfortunately not all details of the tests are known and therefore it is very difficult to estimate the precise amount of produced atmospheric ^{36}Cl. We included tests that took place in the vicinity of sea water, i.e. islands, atolls or barges and had a yield larger than 200 kton, but not the air drop tests. The contributions of tests on islands and atolls were probably lower due to the attenuation of neutron flux by land mass, but not negligible. We calculated the atmospheric input of ^{36}Cl following earlier studies (Elmore et al., 1982; Synal et al., 1990) assuming that 2×10^{26} neutrons are produced by a megaton yield of TNT, that half of the neutrons enter the water and that 32% of those neutrons produce ^{36}Cl (Dyrssen and Nyman, 1955; Machta, 1963). In reality, this value strongly depends on the actual setup of the bomb tests which is not known and is very variable.

Table 1 shows the date and location of the bomb tests as well as the estimated ^{36}Cl produced. It can be seen that the total mass of bomb-produced ^{36}Cl is over 300 kg, which is much more than the 75–80 kg estimated by Elmore et al. (1982) and Synal et al. (1990) from the Dye3 ice core. Fewer tests were taken into account in these earlier works and sometimes the source of information used for the estimation was different in our study. In view of the many uncertainties related to the tests we will use the measured data from different locations world-wide to check the shape and amplitude of the input function. We carry out the simulation using the 310 kg total input of ^{36}Cl from all tests on barges, atolls and islands and then scale the input by comparing the amplitude of modeled fall-out curves with the measured ones. This approach is not perfect but suits the purpose of this study. If the amplitude of the bomb peaks and the fall-out slope of the modeled curves is comparable with the measured curves we assume that the input function is reasonably well defined.

Table 1. Stratospheric bomb produced ^{36}Cl as used as an input for the model simulation. Locations of the bomb test sites: Enewetak atoll (11.35° N, 162.35° E), Bikini atoll (11.30° N, 162.30° E), Johnston island (17.18° N, 169.45° W), Christmas island (2.00° N, 157.25° W), Mururoa atoll, (21.50° S, 138.55° W), Fangataufa atoll (22.15° S, 138.45° W). All tests carried out during one month are summed up in this table.

Year	Month	location	^{36}Cl input* (kg)
1952	10	Enewetak	21
	11	Enewetak	1
1954	2	Bikini	30
	3	Bikini	22
	4	Bikini	15
	5	Bikini	45
1956	6	Bikini	3
	7	Enewetak	4
	7	Bikini	20
1958	5	Bikini	3
	5	Enewetak	3
	5	Enewetak	1
	6	Bikini	2
	6	Enewetak	22
	7	Bikini	19
	7	Enewetak	5
	8	Johnston island	16
1962	4	Christmas island	1
	5	Christmas island	5
	6	Christmas island	30
	7	Johnston island	13
	10	Johnston island	5
1968	7	Mururoa	1
	8	Fangataufa	5
	9	Mururoa	3
1970	5	Mururoa	1
	5	Fangataufa	2
	7	Mururoa	2
	8	Mururoa	1
1971	6	Mururoa	2
	8	Mururoa	3
Total			∼310

* input not yet scaled

The bomb tests produced ^{36}Cl from sea salt on the surface level but the mushroom cloud rose up to the stratosphere. We assumed that all bomb test produced ^{36}Cl reached the stratosphere. The ^{36}Cl that stayed in the troposphere was washed out within a couple of weeks and therefore raised the fluxes only locally and during a short period. For this reason it is of no interest for the simulation.

Table 2. Global means of the measured and modeled accumulation rates (acc.) in water equivalent (the modeled precipitation rates include the standard deviations of the modeled monthly mean values), integrated masses of the ^{36}Cl peaks and the atmospheric residence times corresponding to the fallout slope estimated from the measured and the modeled fluxes. The values are calculated using the scaled ^{36}Cl input (∼80 kg).

Site units	location	altitude	acc. meas. mm/day	acc. mod. mm/day	mass meas. kg	mass mod. kg	res. time meas. years	res. time mod. years
Dye3	65° N, 48° W	2480 m	1.5	1.5±0.9	70	55	4.2	3.7
Fiescherhorn	46° N, 8° E	3900 m	4	2.3±1.1	75	120	3.6	4.0
Grenzgletscher	46° N, 7° E	4200 m	5	2.8±1.4	100	120	3.5	4.0
Guliya	35° N, 83° E	6710 m	0.8	0.8±0.8	40	140	4.1	4.2
Huascaran	9° S, 77° W	6050 m	3	3.3±2.7	80	80	5.6	7.0
NGRIP	75° N, 43° W	2917 m	0.5	0.5±0.3	34	28	3.4	3.7
Tien Shan	42° N, 80° W	5000 m	4	0.3±0.3	240	120	5.9	4.6
Berkner Island	79° S, 47° W	900 m	0.4	0.3±0.3	14	10	–	–

The height and radius of the mushroom cloud was calculated following Glasstone and Dolan (1977) (their Fig. 2.16). The cloud radius varied between 6 and 30 km depending on the strength of the bomb but still the radius was smaller than the grid box size of the model. However, the cloud was initialized over 9 horizontal grid points and 4 vertical levels of the model and read in within two time steps to reduce the extreme gradients of the ^{36}Cl concentrations between the neighbouring grid boxes. Only tests with a yield larger than 200 kton were considered for the simulation because these gave a cloud height large enough to place the produced ^{36}Cl into the stratosphere.

4 Results

4.1 The total mass of the bomb test produced ^{36}Cl

Table 2 shows the total masses of the bomb test produced ^{36}Cl integrated from the measured and the modeled ^{36}Cl deposition flux peaks. The masses were calculated assuming that the peak in question was representative of the global mean fallout rate in order to estimate the global total input of bomb produced ^{36}Cl. The integration was performed trying to avoid the fact that the total mass of the peak might depend on one single data point which might be erroneous.

All modeled fluxes were consequently larger than the measured fluxes. Thus we chose to scale the modeled input of ^{36}Cl down by a factor of 4, giving the best agreement between the modeled and measured deposition fluxes worldwide. All results presented in this manuscript are calculated using the scaled input of ∼80 kg. It has to be kept in mind that due to the loss of gaseous ^{36}Cl in firn (see Sect. 2) the measured fluxes represent a lower limit. Because the ^{36}Cl fluxes showed a steep leading edge of the bomb peak in all data sets, we assume that the loss in these ice cores was negligible. This is likely due to the relatively high accumulation rate at all ice core sites.

It seems that the deposition flux measured at the Dye3 site represents well the global mean deposition flux of the bomb produced ^{36}Cl, because the integrated mass of ∼70 kg agrees with the assumed total input of ∼80 kg calculated by Elmore et al. (1982) and Synal et al. (1990) from the measured ^{36}Cl flux in the Dye3 ice core.

4.2 Measured and modeled ^{36}Cl deposition fluxes

Figure 2 summarizes the modeled and measured ^{36}Cl deposition flux peaks and Fig. 3 shows the individual sites. The temporal resolution of the measured fluxes varies between one and several years depending on the core. We show the annual means of the modeled fluxes on a logarithmic scale to be able to compare the fallout slopes of the curves. The slope is a measure of the shape of the bomb produced input function of ^{36}Cl and the sinks. The agreement between the measured and the modeled slopes in Figs. 2 and 3 and Table 2, indicates that the shape of the input function is reasonable. This means that the estimated amount of ^{36}Cl produced by the individual tests is reasonably defined regardless of the many uncertainties.

The measured and modeled fluxes in Fig. 2 all show a very similar declining trend with a maximum around 1955–1956. Only the measured peak at Huascarán exhibits a maximum earlier than this, around 1951–1952. A possible explanation is the high altitude location of the Huascarán site (>6000 m). The site could have experienced a strong intrusion of stratospheric air shortly after the bomb test which the model does not reproduce. However this maximum is represented by only one data point with poor age control and should be interpreted with care. It could also be related to an uncertain dating. The fact that the maximum of the ^{36}Cl measured at Dye3 shows up a couple of years later than in the other cores is harder to explain. The Dye3 ice core is the best dated (annual resolution) meaning that the later occurrence of the maximum is probably related to some local scale processes rather than to dating problems. Different transport paths of

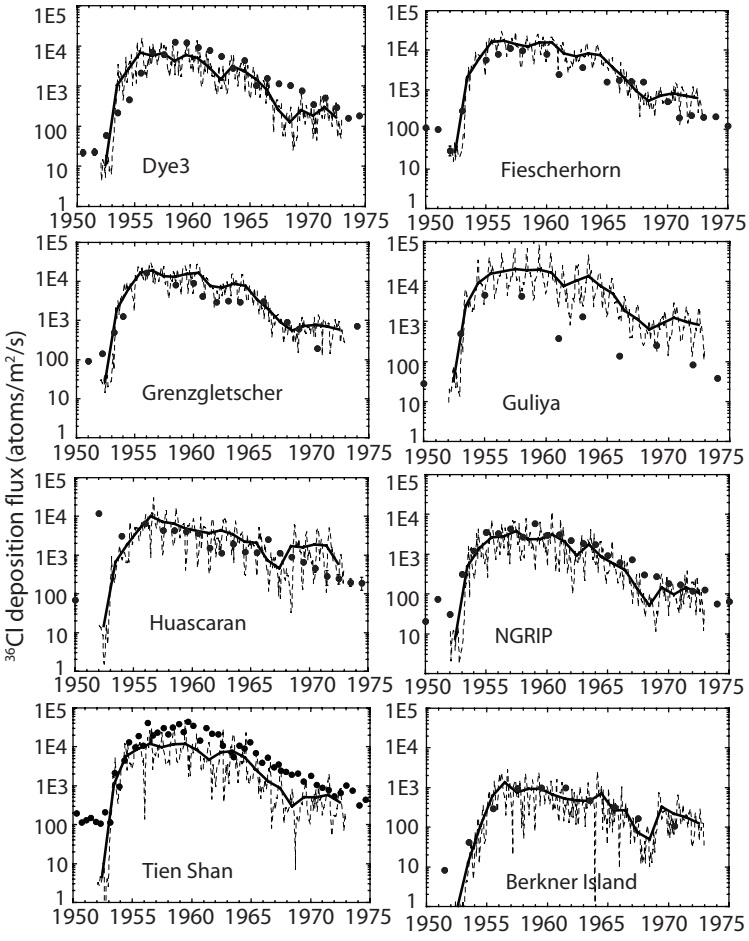

Fig. 3. Deposition fluxes of ^{36}Cl (atoms/m^2/s) in the analyzed ice cores. The dots represent the measured values with their measurement errors which are hardly visible on the logarithmic scale. The dashed narrow line shows the modeled monthly mean fluxes and the thick full line the annual means of the modeled fluxes.

^{36}Cl to polar regions cannot be the reason for the discrepancy because the ^{36}Cl measured in the NGRIP core exhibits the maximum simultaneously with the tropical or mid-latitude cores. The maximum is reached later at the Berkner Island site because of the resublimation of gaseous ^{36}Cl from firn, as discussed in Sect. 2.

The measured flux at the Guliya site is clearly lower than those of the other mid-latitude cores. Because the measured ^{36}Cl concentrations in ice were comparable in all ice cores including Guliya, the much lower fluxes can probably be explained by the quite low accumulation rate of 0.8 mm/day W. E. compared with other sites. It has to be kept in mind that at Guliya some of the snow might be lost due to strong winds so that the measured snow accumulation rate represents rather a lower limit. The escape of the gaseous ^{36}Cl in firn mentioned earlier (see Sect. 2) is not a probable explanation because the snow accumulation rate at Guliya is relatively high compared with the critical value of 0.1 mm/day estimated by Röthlisberger et al. (2003).

Next we address the question how well the modeled fluxes agree with measurements. Figure 3 compares the modeled ^{36}Cl deposition fluxes with the measured values in all ice cores. The dashed line shows the modeled monthly mean values and the thick line the annual means. The dots depict the measured values with their measurement errors (mostly between 5 and 20%) which are almost invisible on the logarithmic scale.

Generally the modeled fluxes agree quite well with the measured fluxes. At all ice core sites except Guliya and to a smaller extent Tien Shan the model is able to capture the correct level of the peaks reasonably well. At Dye3, the measured and modeled fluxes agree quite well except the fact that the maximum of the measured flux occurs later, as discussed above. Fiescherhorn and Grenzgletscher are both located in the Swiss Alps and fall within the neighbouring grid boxes of the model. The measured fluxes are very similar in magnitude. The calculated total masses of the peaks differ by some 25%. At both locations the model somewhat overestimates the measured fluxes.

Guliya is the only site where the model significantly overestimates the measured flux. This is probably a combination of loss of snow on the mountain due to winds and overestimation of the modeled deposition flux. The modeled precipitation rate agrees very well with the one measured from the ice core and is also comparable with the range of 0.4–0.7 mm/day for the years 1990–1991 given by Thompson et al. (1995a). If however some snow was lost due to winds, the model would underestimate the actual precipitation rate. A marked seasonal variability in the ^{36}Cl flux, as shown by the thin dashed line in Fig. 3, reflects the strong influence of monsoon on the area (Thompson et al., 1995a). It follows the modeled precipitation rate which also varies more than at the other ice core sites (see the standard deviations in Table 2). Another difference to other sites is the very high altitude of the Guliya site (6710 m) which cannot be resolved by the model. Therefore the modeled precipitation rate at Guliya is representative for lower altitudes.

As mentioned before, the ^{36}Cl flux measured in the Huascarán ice core shows a maximum 2–3 years before the other cores but this maximum is represented only by one data point. Otherwise the agreement between the measured and modeled fluxes is good. The large seasonal variability reflects the seasonal movement of the intertropical convergence zone with a precipitation rate which is high in summer and low in winter.

At NGRIP the agreement between the modeled and measured flux is good and both fluxes exhibit a maximum at the same time. The fluxes measured and modeled at NGRIP are very low due to the low precipitation rate at the site and because little stratospheric air reaches these high latitudes.

At Tien Shan the model somewhat underestimates the measured flux. The flux measured in this ice core is significantly larger than at other sites which is also reflected by the total mass of the peak in Table 2. At Tien Shan the increase from the natural level to the bomb produced level is very steep and agrees best with the modeled increase. The steep increase can be explained by the highest temporal resolution of the Tien Shan ice core and probably also by the mid-latitude location of the site, which can experience intrusions of stratospheric air.

The agreement between the measured and modeled flux at the Berkner Island site is relatively good regardless of the flattening of the measured curve due to sublimation of gaseous ^{36}Cl from firn. This confirms that the sublimation is not a serious problem in the Berkner Island ice core. The flatter increase from the natural level to the bomb produced level is partly due to this phenomenon but more due to the different transport paths to the Antarctic continent, reflected by the slower increase of the modeled flux (see Fig. 4).

The modeled precipitation rates shown in Table 2 agree quite well with those calculated from the snow accumulation rates of the ice cores. No direct precipitation rate observations exist from the Guliya, Huascarán, Tien Shan or Berkner Island sites nor from the two Alpine glaciers. The precipitation rates calculated from the snow accumulation of the Alpine ice cores agree generally well with the values measured at a near-by high-altitude Alpine station Jungfraujoch (3.5 mm/day W.E.) (Heikkilä et al., 2008b). The measured precipitation rate at Jungfraujoch represents a lower limit because the collector is mounted on a ridge and some of the snow is blown over it. A comparison of stable isotope data, a proxy for precipitation, from Jungfraujoch and Fiescherhorn reveals a very similar behavior between Jungfraujoch and Fiescherhorn (Schotterer et al., 1997b). The modeled rates are slightly lower than the ones calculated from the snow accumulation but the uncertainty is within a factor of 2 and also the modeled precipitation rate at Grenzgletscher is larger than at Fiescherhorn, in agreement with the calculated rates. At Tien Shan the model very largely underestimates the precipitation rate calculated from the ice core (modeled 0.3 mm/day, measured 4 mm/day). The reason for this is unknown. The ability of ECHAM5-HAM model to reproduce the observed precipitation rates world-wide has been largely discussed in Hagemann et al. (2006) and shows that the error on scales of a couple of hundred of kilometers is never larger than 100%. Comparison of the observed precipitation rates from the CMAP observational reanalysis data set in Hagemann et al. (2006) shows that also the observed precipitation rate in the Tien Shan region is less than 1 mm/day when averaged over a larger region. No direct observations from this region exist, meaning that also the quality of the CMAP data depends strongly on the algorithms used to derive the precipitation rates from satellite measurements (Hagemann et al., 2006). We assume that the Inylchek glacier in the Tien Shan mountains experiences locally much higher precipitation than the surrounding valleys. It is known that in the mountains the local precipitation rate depends strongly on the origin of air masses and can vary locally. Such local effects are impossible to resolve within the model grid size of a couple of hundred kilometers.

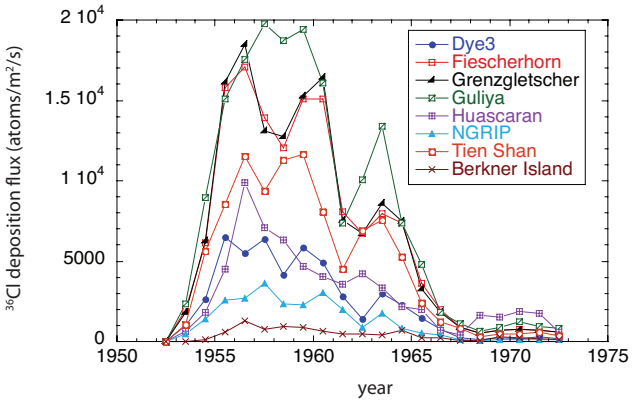

Fig. 4. The modeled annual mean ^{36}Cl deposition fluxes (atoms/m^2/s) on a linear scale at the ice core sites.

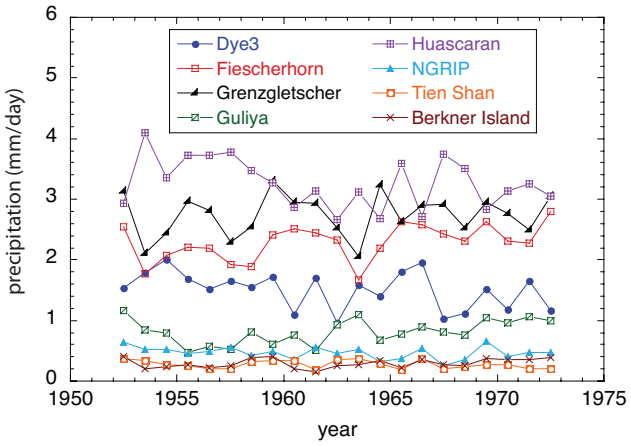

Fig. 5. The modeled annual mean precipitation rates (mm/day water equivalent) at the ice core sites.

In order to compare the different ice cores with each other we show the modeled annual mean ^{36}Cl fluxes on a linear scale (Fig. 4). The fluxes at all ice core sites exhibit a maximum between 1955 and 1960. At Guliya the maximum occurs two years later than at other sites but reflects the enormous seasonal variability so that the high values during 1957–1959 are caused by one single month of very high deposition. The fluxes at Fiescherhorn and Grenzgletscher behave in a very similar way and quickly drop down during 1957 and 1958 after the peak of 1955–1956 and then rise again during 1959 and 1960. This drop seems to follow the drop in the precipitation rate, shown in Fig. 5, before new large test series started in 1958. The modeled bomb peak at Huascarán and Berkner Island, the only southern hemispheric sites, are somewhat different from the modeled peaks in the Northern Hemisphere. The maximum at both sites is reached in 1956, when the precipitation rate is similar to earlier years. This is about a year later than at the other sites and probably reflects the fact that the bomb tests took place in the Northern Hemisphere and more time was required until the ^{36}Cl atoms reached the other hemisphere. The French atom bomb tests starting 1968 at Mururoa and Fangataufa atolls were the only tests performed in the Southern Hemisphere. These tests can clearly be seen as a maximum in the Huascarán and Berkner Island fluxes but are much less visible in the northern hemispheric sites. These tests took place in the southern hemispheric winter months (May to September) during which the Brewer-Dobson circulation very efficiently transports the ^{36}Cl atoms towards the southern high latitudes so that not much ^{36}Cl reaches the Northern Hemisphere. The peak at Huascarán occurs in 1968/1969 and slightly later at Berkner Island again reflecting the longer transport path to Antarctica.

4.3 Latitudinal dependence of the bomb peaks of ^{36}Cl fluxes

It is interesting to consider how the amplitude of the ^{36}Cl bomb peak depends on the location of the ice core and the role of the local precipitation rate and latitude of the site. We have animated the zonal and monthly mean ^{36}Cl concentrations which show the location of the bomb produced ^{36}Cl input into the stratosphere and its mixing and transport to the troposphere. Further animations illustrate the monthly mean deposition of ^{36}Cl globally as well as in Greenland and Antarctica. The animations are provided as supplement for this manuscript.

Figure 4 shows that the modeled bomb peaks are largest at Guliya (35° N), Tien Shan (42° N), Fiescherhorn and Grenzgletscher (46° N), located in the subtropics-midlatitudes where the stratosphere-troposphere air exchange is strongest at the subtropical tropopause breaks (Holton et al., 1995; Stohl et al., 2003). The large precipitation rates at the two Swiss alpine sites probably also increase the ^{36}Cl deposition but not at Guliya or Tien Shan where the modeled precipitation rate is quite low. At Dye3 the precipitation rate is quite high which leads to a rather large bomb peak although the direct influence of stratospheric air is lower at 65° N. The modeled bomb peak at Huascarán is also low although the modeled precipitation rate is the largest. The Huascarán site is located close to the equator (9° S) so that less stratospheric air reaches the site than in the subtropics. The peak is lowest at Berkner Island site (79° S) because of the very low precipitation rate and because little stratospheric air reaches high latitudes.

The modeled global annual mean deposition flux of ^{36}Cl suggests (see the animated global deposition flux) that the bomb peak is visible all around the globe, even in very dry areas. This is confirmed by the observable, though low, bomb peak measured and modeled at the Berkner Island site. Independent of the ^{36}Cl concentration in the atmosphere the wet deposition is always dominant (>90%) except in very dry areas (central Antarctica, Sahara, west of the African and South American continents) where the fraction of dry deposition can be above 50% at largest.

Figure 6 illustrates the time evolution of the zonal and annual mean ^{36}Cl deposition fluxes. The peaks are larger in the Northern Hemisphere in the fifties and sixties because the bomb tests took place in the Northern Hemisphere and also, after the hemispheric mixing of the stratosphere, reflect the stronger stratosphere-troposphere exchange in the Northern Hemisphere. Because of this the fluxes are consequently lower by ∼20% in the Southern Hemisphere than in the Northern Hemisphere. The peaks are larger in the Southern Hemisphere following the French bomb tests there commencing in 1968. The maxima of the fluxes occur in the midlatitudes, between 30° and 50° in both hemispheres reflecting the stratospheric origin of the bomb produced ^{36}Cl. In the tropics there is another smaller maximum caused by the

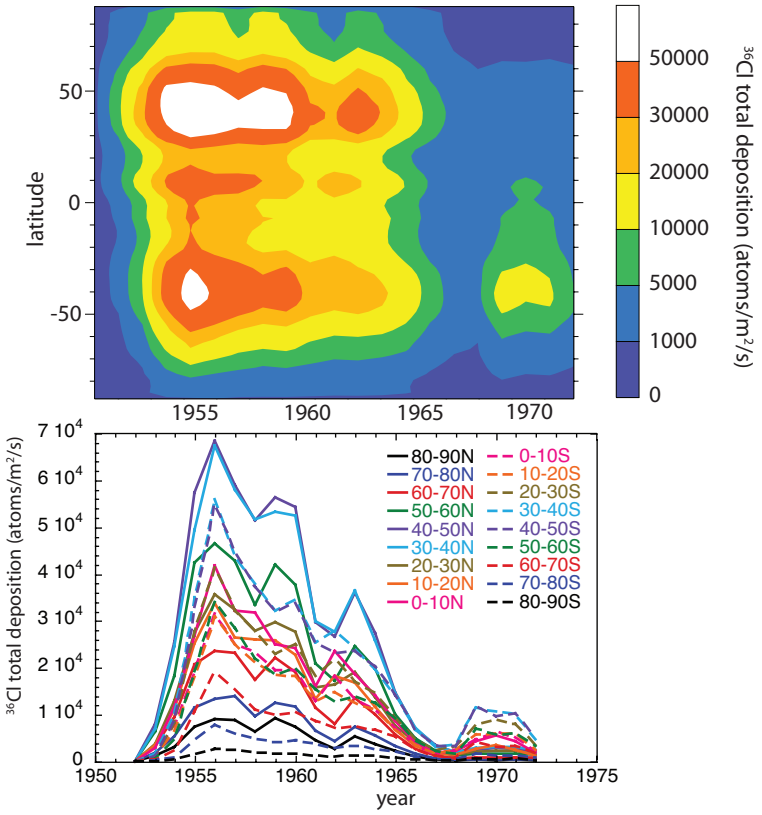

Fig. 6. The time evolution of the modeled annual zonal mean ^{36}Cl deposition fluxes (above). The time evolution of the modeled annual zonal mean ^{36}Cl deposition fluxes averaged over 10-degree latitude bands (below).

extreme precipitation rates in the intertropical convergence zone. The fluxes are lowest in the polar latitudes (70°–90°) where the difference to the midlatitude fluxes is a factor of 5–6. The Southern Hemisphere test peak starting in 1968 is well visible in the Southern Hemisphere fluxes and to some extent in the Northern Hemisphere low latitudes.

4.4 Stratospheric residence time of bomb produced ^{36}Cl

Most general circulation models overestimate the vertical transport of tracers, leading to an underestimation of stratospheric residence time and concentrations (Mahowald et al., 2002). Simulations of stratospheric tracers made with ECHAM4/5-HAM also point to this problem (Timmreck et al., 1999; Heikkilä et al., 2008a). Therefore it is of importance to investigate the extent the model underestimates the stratospheric residence time of ^{36}Cl and so the fallout pattern in the ^{36}Cl deposition fluxes.

The average slopes of the fallout curves from the different ice cores are shown in Table 2, except for the Berkner Island core because the fall-out pattern is unrealistically flat, due to the mobility of gaseous ^{36}Cl in firn. They have been calculated as the slope of the logarithmic fallout curve but we show the corresponding atmospheric residence time. The fallout curves do not show the correct residence times due to the repeated input of ^{36}Cl due to new tests but rather reflect the steepness of the slopes.

The slopes are very similar if calculated from the modeled fluxes. The mean residence time of ^{36}Cl at all ice core locations is 3–4 years except at Huascarán (5–6 years) and Tien Shan (5–6 years). The flatter fallout of the ^{36}Cl fluxes at Huascarán is due to the later southern hemispheric bomb tests which contribute more to the Southern Hemisphere core. The modeled slope is even flatter (corresponding to a residence time of 7 years) because the modeled increase in the deposition flux is larger than in the measured flux. This might indicate that the estimated input from the latest tests is slightly too large but because we have data from only two southern hemispheric ice cores it is too early to draw strong conclusions. The residence time given by the fallout curve of ^{36}Cl (3–4 years) is longer than the assumed stratospheric residence time of cosmogenic ^{10}Be or ^{36}Cl of ∼1 years (Sachsenhauser et al.[1]) because the slope is flattened by the repeated tests which raise the deposition fluxes during the later years. The stratospheric residence time can be estimated during years when no additional tests took place. For example in 1962–1968 when no additional tests took place the slope

[1]Sachsenhauser, H., Zerle, L., Beer, J., Masarik, J., and Nolte, E., Atmospheric transport of cosmogenic radionuclides, Wengen

of the modeled fallout is a bit steeper than the measured flux at least in the Dye3 core. This is caused by the overestimated downward transport of the model, mentioned above. The residence time estimated from the modeled fluxes between 1964 and 1968 varies between 1.3 and 1.7 years, which is slightly shorter than the estimated residence time of 2±0.3 years from the Dye3 core by Synal et al. (1990) between 1960 and 1964 when no tests took place in their estimated input function. The other measured fluxes are not optimal for the residence time estimation during these years because of their coarser temporal resolution. The NGRIP data has an annual resolution but does not show a steeper drop-off rate during this period. The Tien Shan data has an even higher than annual resolution which makes it difficult to distinguish between a steeper drop-off rate or seasonal variability.

Another reason for the longer residence time of bomb produced ^{36}Cl compared with the ∼1 year estimated by Sachsenhauser et al.[1] is the very different input distribution of natural and bomb produced ^{36}Cl. Whereas the cosmogenic ^{36}Cl is produced mostly at high latitudes due to geomagnetic shielding of cosmic rays in the atmosphere, the bomb input takes place in the tropical stratosphere. Following the Brewer-Dobson circulation the bomb produced ^{36}Cl is transported towards the high latitudes before it sinks and is transported to the troposphere in the subtropics where the stratosphere-troposphere exchange is most efficient (Holton et al., 1995; Stohl et al., 2003). This leads to a longer stratospheric transport path than the cosmogenic ^{36}Cl which is produced in the high latitude stratosphere.

5 Summary and conclusions

The bomb test produced deposition peak of ^{36}Cl, observed in ice cores world-wide was used to investigate the ability of the ECHAM5-HAM general circulation model to simulate the stratospheric transport and residence time of ^{36}Cl. We modeled a 21-year period from the beginning of the atmospheric bomb tests in 1952 until 1972. All tests that produced ^{36}Cl took place in the tropics. Comparison of the ice core ^{36}Cl deposition fluxes with the modeled deposition fluxes indicate that the total input of bomb produced ^{36}Cl into the atmosphere was ∼80 kg, in agreement with previous studies. There are differences in the amplitude of the bomb peaks from different cores depending on their latitude as well as the precipitation rate at the drilling site.

The modeled fallout pattern of the ^{36}Cl deposition fluxes agrees generally well with the measured fluxes in the Dye3, Fiescherhorn, Grenzgletscher, Huascarán and NGRIP ice cores. At Tien Shan site the model somewhat underestimates the measured flux. In the case of the Guliya core the modeled flux was significantly larger than the measured flux. There was a consequent offset of the modeled flux during the whole modeled period but the fallout pattern was very similar in both the modeled and the measured flux. The modeled precipitation rate at Guliya agreed mostly well with the precipitation rate calculated from the snow accumulation rate of the core. The modeled flux at Guliya was very large due to the location of the Guliya site in the subtropics where the stratosphere-troposphere exchange is largest. The Guliya site is also influenced by the monsoon which leads to an extremely large seasonal variability in the precipitation and therefore deposition of ^{36}Cl. The rather low measured ^{36}Cl flux at Guliya might be explained by the fact that some of the snow is lost due to strong winds in the Guliya plateau.

At other drilling sites the agreement between the modeled and measured fluxes was quite good. In the Dye3 ice core the observed maximum occured later than in the modeled flux which is probably caused by some local scale processes because the dating of the Dye3 core is reliable. The ^{36}Cl flux at Huascarán and Berkner Island, which are the only southern hemispheric ice cores, clearly show the French bomb tests which took place in the end of the sixties and seventies in the Southern Hemisphere. The ^{36}Cl fluxes in the northern hemispheric cores do not show these tests as clearly.

An animation of the ^{36}Cl concentrations in the atmosphere shows that the extent and speed of mixing between the hemispheres depends on the season of the test. The ^{36}Cl produced by the tests in wintertime is more efficiently transported towards the pole which leads to a weaker signal in the opposite hemisphere. The animated world-wide deposition flux of bomb produced ^{36}Cl shows that the fallout of bomb produced ^{36}Cl is largest in the subtropics and midlatitudes where the air exchange between the stratosphere and the troposphere is strongest, but also in the tropics due to the high precipitation rate. In Greenland the fallout is slightly smaller in amplitude than in the mid-latitudes whereas in Antarctica the signal is significantly smaller. In polar regions, both in Greenland and in Antarctica, the amplitude of the bomb peak depends on the precipitation rate, which varies so much locally that the quantification of the amplitude of the peak is very difficult. The results indicate that the bomb peak should be clearly visible everywhere on the Earth, even in the driest areas.

The fallout pattern, both modeled and measured, reveal a very similar slope, which corresponds to a residence time in the order of 3–4 years. This slope does not directly show the atmospheric residence time of the bomb produced ^{36}Cl because of the repeated input of ^{36}Cl into the stratosphere caused by new tests, which flattened the fallout pattern of the deposition fluxes. The good agreement between the modeled and the observed slopes indicates that the form of the input function of the bomb produced ^{36}Cl is reasonably well reconstructed. The modeled stratospheric residence times of ^{36}Cl during a period when no new tests took place are 1.3–1.7 years, which are slightly lower than the ∼2 years estimated from the Dye3 ice core. This means that although the middle atmospheric version of ECHAM5-HAM somewhat overestimates the stratosphere-troposphere exchange it still does a reasonable job in simulating the transport and atmospheric residence times of stratospheric tracers.

Acknowledgements. We would like to thank the German Computing Center (DKRZ) for providing us with the computing time. This work is financially supported by the NCCR climate. We are grateful to S. Bollhalder Lück and I. Brunner for preparing the ^{36}Cl samples. We acknowledge Christoph Wirz for providing information on the bomb tests. We would also like to thank A.-M. Berggren for proof-reading the manuscript.

Edited by: U. Baltensperger

References

Andersen, K. K., Ditlevsen, P. D., Rasmussen, S. O., Clausen, H. B., Vinther, B. M., Johnsen, S. J., and Steffensen, J. P.: Retrieving a common accumulation record from Greenland ice cores for the past 1800 years, J. Geophys. Res., 111, D15106, doi:10.1029/2005JD006765, 2006.

Blinov, A. Massonet, S., Sachsenhauser, H., Stan-Sion, C., Lazarev, V., Beer, J., Synal, H.-A., Kaba, M., Masarik, J., and Nolte, E.: An excess of ^{36}Cl in modern atmospheric precipitation, Nucl. Inst. Meth. Phys. Res. B, 172, 537–544, 2000.

Davis, S., Cecil, L. D., Zreda, M., and Moysey, S.: Chlorine-36, bromide and the origin of spring water, Chem. Geol., 179, 3–16, 2001.

Delmas, R. J., Beer, J., Synal, H.-A., Muscheler, R., Petit, J.-R., and Pourchet, M.: Bomb-test ^{36}Cl measurements in Vostok snow (Antarctica) and the use of ^{36}Cl as a dating tool for deep ice cores, Tellus, 56B, 492–498, 2004.

Dentener, F., Kinne, S., Bond, T., Boucher, O., Cofala, J., Generoso, S., Ginoux, P., Gong, S., Hoelzemann, J. J., Ito, A., Marelli, L., Penner, J. E., Putaud, J.-P., Textor, C., Schulz, M., van der Werf, G. R., and Wilson, J.: Emissions of primary aerosol and precursor gases in the years 2000 and 1750 prescribed data-sets for AeroCom, Atmos. Chem. Phys., 6, 4321–4344, 2006, http://www.atmos-chem-phys.net/6/4321/2006/.

Dyrssen, D. and Nyman, P. O.: Acta Radiol., 43, 421–427, 1955.

Eichler, A., Schwikowski, M., Gäggeler, H., Furrer, V., Synal, H.-A., Beer, J., Saurer, M., and Funk, M.: Glaciochemical dating of an ice core from upper Grenzgletscher (4200 m a.s.l.), J. Glaciol., 46, 507–515, 2000.

Elmore, D., Tubbs, L. E., Newman, D., Ma, X. Z., Finkel, R., Nishizumi, K., Beer, J., Oescher, H., and Andree, M.: ^{36}Cl bomb pulse measured in a shallow ice core from Dye3, Greenland, Nature, 300, 735–737, 1982.

Gates, W. L.: AMIP: The Atmospheric Model Intercomparison Project, B. Am. Meteorol. Soc., 73, 1962–1970, 1992.

Glasstone, S. and Dolan, P. J.: The effects of nuclear weapons, United States Department of Defense and Energy Research and Development Administration, 3rd Edition, 1977.

Green, J. R., Cecil, L. D., Synal, H.-A., Santos, J., Kreutz, K. J., and Wake, C. P.: A high resolution record of chlorine-36 nuclear-weapons-tests fallout from Central Asia, Nucl. Instrum. Meth. B, 223–224, 854–857, 2004.

Field, C., Schmidt, G., Koch, D., and Salyk, C.: Modeling production and climate-related impacts on ^{10}Be concentration in ice cores, J. Geophys. Res. 111, D15107, doi:10.1029/2005JD00640, 2006.

Hagemann, S., Arpe, K., and Roeckner, E.: Evaluation of the hydrological cycle in the ECHAM5 model, J. Climate, 19, 16, 3810–3827, 2006.

Heikkilä, U., Beer, J., and Feichter, J.: Modeling cosmogenic radionuclides 10Be and 7Be during the Maunder Minimum using the ECHAM5-HAM General Circulation Model, Atmos. Chem. Phys., 8, 2797–2809, 2008a, http://www.atmos-chem-phys.net/8/2797/2008/.

Heikkilä, U., Beer, J., and Alfimov, V.: Beryllium-10 and Beryllium-7 in precipitation in Dübendorf (440 m) and at Jungfraujoch (3580 m), Switzerland (1998–2005), J. Geophys. Res., 113, D11104, doi:10.1029/2007JD009160, 2008b.

Holton, J., Haynes, P., McIntyre, M., Douglass, A., Rood, R., and Pfister, L.: Stratosphere-troposphere exchange, Rev. Geophys., 33, 403–439, 1995.

Lal, D. and Peters, B.: Cosmic ray produced radioactivity on the Earth, Handbuch der Physik, XLVI/2, Springer-Verlag, New York, 551–612, 1967.

Lukasczyk, C.: ^{36}Cl im Grönlandeis, Diss. ETH No. 10688, http://e-collection.ethbib.ethz.ch/eserv/eth:22378/eth-22378-02.pdf, 201–203, 1994 (in German).

Machta, L.: Radioactive fallout from nuclear weapons tests, US-AEC, Oak Ridge, 369–391, 1963.

Mahowald, N., Plumb, A., Rasch, P., del Corral, J., Sassi, F., and Heres, W.: Stratospheric transport in a three-dimensional isentropic coordinate model, J. Geophys. Res., 107(D15), 4254, doi:10.1029/2001JD001313, 2002.

Masarik, J. and Beer, J.: Simulation of particle fluxes and cosmogenic nuclide production in the Earth's atmosphere, J. Geophys. Res., 104, 12099–12111, 1999.

North Greenland Ice Core Project Members, High-resolution record of Northern Hemisphere extending into the last interglacial period, Nature, 431, 147–151, 2004.

Rehfeld, S. and Heimann, M.: Three dimensional atmospheric transport simulation of the radioactive tracers ^{210}Pb, ^{7}Be, ^{10}Be and ^{90}Sr, J. Geophys. Res., 100(D12), 26141–26161, 1995.

Roeckner, E., Baeuml, G., Bonventura, L., Brokopf, R., Esch, M., Giorgetta, M., Hagemann, S., Kirchner, I., Kornblueh, L., Manzini, E., Rhodin, A., Schlese, U., Schulzweida, U., and Tompkins, A.: The atmospheric general circulation model ECHAM5. PART I: Model description, Report 349, Max Planck Institute for Meteorology, Hamburg, Germany, available at: http://www.mpimet.mpg.de, 2003.

Röthlisberger, R., Mulvaney, R., Wolff, E. W., Hutterli, M. A., Bigler, M., de Angelis, M. Hansson, M. E., Steffensen, J. P., and Udisti, R.: Limited dechlorination of sea-salt aerosols during the last glacial period: Evidence from the European Project for Ice Coring in Antarctica (EPICA) Dome C ice core, J. Geophys. Res. 108(D16), 4526, doi:10.1029/2003JD003604, 2003.

Schlosser, P., Stute, M., Dörr, H., Sonntag, C., and Münnich, K. O.: Tritium/^{3}He dating of shallow groundwater, Earth Planet. Sci. Lett., 89, 353–362, 1988.

Schotterer, U., Schwarz, P. and Rajner, V.: From pre-bomb levels to industrial times: A complete tritium record from an alpine ice core and its relevance for environmental studies, IAEA-SM-349/55, 1997a.

Schotterer, U., Fröhlich, K., Gäggeler, H. W., Sandjordj, S., and Stichler, W.: Isotope records from Mongolian and Alpine ice cores as climate indicators, Clim. Change, 36, 519–530, 1997b.

Schwikowski, M., Brütsch, S., Gäggeler, H., and Schotterer, U.: A high-resolution air chemistry record from an Alpine ice core:

Fiescherhorn glacier, Swiss Alps, J. Geophys. Res., 104(D11), 13709–13719, 1999.

Steinhilber, F., Abreu, J. A., and Beer, J.: Solar modulation during the Holocene, Astrophys. Space Sci. Trans., 4, 1–6, 2008, http://www.astrophys-space-sci-trans.net/4/1/2008/.

Stier, P., Feichter, J., Kinne, S., Kloster, S., Vignati, E., Wilson, J., Ganzeveld, L., Tegen, I., Werner, M., Balkanski, Y., Schulz, M., Boucher, O., Minikin, A., and Petzold, A.: The aerosol-climate model ECHAM5-HAM, Atmos. Chem. Phys., 5, 1125–1156, 2005, http://www.atmos-chem-phys.net/5/1125/2005/.

Stohl, A., Bonasoni, P., Cristofanelli, P., Collins, W., Feichter, J., Frank, A., Forster, C., Gerasopoulos, E., Gäggeler, H., James, P., Kentarchos, T., Kromp-Kolb, H., Krüger, B., Land, C., Meloen, J., Papayannis, A., Priller, A., Seibert, P., Sprenger, M., Roelofs, G. J., Scheel, H.E., Schnabel, C., Siegmund, P., Tobler, L., Trickl, T., Wernli, H., Wirth, V., Zanis, P., and Zerefos, C.: Stratosphere–troposphere exchange: A review, and what we have learnt from STACCATO, J. Geophys. Res., 108(D12), 8516, doi:10.1029/2002JD002490, 2003.

Synal, H.-A., Beer, J., Bonani, G., Suter, M., and Wölfli, W.: Atmospheric transport of bomb-produced ^{36}Cl, Nucl. Instr. Meth., B52, 483–488, 1990.

Thompson, L. G., Mosley-Thompson, E., Davis, M. E., Lin, P. N., Dai, J., Bolzan, J. F., and Yao, T.: A 1000 year climate ice-core record from the Guliya ice cap, China: its relationship to global climate variability, Ann. Glaciol., 21, 175–181, 1995a.

Thompson, L. G., Mosley-Thompson, E., Davis, M. E., Lin, P.-N., Henderson, K. A., Cole-Dai, J., Bolzan, J. F., and Liu, K.-B.: Late glacial stage and Holocene tropical ice core records from Huascarán, Peru, Science, 269, 46–50, 1995b.

Thompson, L. G., Mosley-Thopson, E., Davis, M. E., Henderson, K. A., Brecher, H. H., Zagorodnov, V. S., Mashiotta, T. A., Ping-Nan, L., Mikhalenko, V. N., Hardy, D. R., and Beer, J.: Kilimanjaro ice core records: evidence of Holocene climate change in tropical Africa, Science, 289, 589–593, doi:10.1126/science.1073198, 2002.

Timmreck, C., Graf, H.-F., and Feichter, J.: Simulation of Mt. Pinatubo volcanic aerosol with the Hamburg Climate Model ECHAM4, Theor. Appl. Climatol., 62, 85–108, 1999.

Usoskin, I. G., Alanko–Huotari, K., Kovaltsov, G. A., and Mursula, K.: Heliospheric modulation of cosmic rays: Monthly reconstruction of 1951–2004, J. Geophys. Res., 110, A12108, doi:10.1029/2005JA011250, 2005.

Zerle, L., Faestermann, T., Knie, K., Korschinek, G., Nolte, E., Beer, J., and Schotterer, U.: The ^{41}Ca bomb pulse and atmospheric transport of radionuclides, J. Geophys. Res., 102(D16), 19517–19527, 1997.